ChemComm

RSC Publishing

COMMUNICATION

View Article Online
View Journal | View Issue

# Injection synthesis of Ni–Cu@Au–Cu nanowires with tunable magnetic and plasmonic properties†

Cite this: *Chem. Commun.*, 2013, **49**, 11545

Received 30th July 2013,
Accepted 16th October 2013

DOI: 10.1039/c3cc45800h

www.rsc.org/chemcomm

Deqian Zeng, Yuanzhi Chen,* Aolin Lu, Meng Li, Huizhang Guo, Junbao Wang and Dong-Liang Peng*



**A facile nonaqueous injection method has been developed for the construction of one-dimensional nanostructure consisting of a magnetic alloy (Ni–Cu) core and a plasmonic alloy (Au–Cu) shell. The obtained Ni–Cu@Au–Cu nanowires exhibit tunable optical and magnetic properties.**

In recent years, metallic core–shell nanostructures have attracted a tremendous amount of research interest due to their potential applications in a variety of fields such as catalysis,[1–3] nanoelectronics,[4] transparent conductors,[5] microwave absorption,[6] chemical sensing[7] and magnetic resonance imaging (MRI) enhancement.[8,9] Among them, the metallic nanowires with a core–shell structure are especially attractive. Compared to monometallic nanowires, core–shell structured nanowires are characterized by the radial variation in composition and microstructure, thus they possess additional or enhanced properties that are not possessed by their monometallic counterparts or even new properties due to synergistic effects between different components. As a result, considerable efforts have been made towards the synthesis, structural characterization and property exploration of core–shell structured metallic nanowires.[5,10–15] The improved or new features obviously bring advantages for particular applications. For example, Cu nanowires have been demonstrated to be a low-cost alternative for Ag in transparent conducting films that have wide application in displays, solar cells, organic light-emitting diodes, and electrochromic windows. However surface oxidation hinders their practical applications. The incorporation of Ni to form an alloy shell allows the production of core–shell nanowires that are highly resistant to oxidation.[5] In addition, if the shell of a nanowire contains a noble metal such as Au, it will furnish new functionalities to expand its applications. However, it is not easy to coat a noble metal shell over a magnetic metal core *via* common solution methods. Reports on the preparation of magnetic@noble alloy nanowires are also very rare.

*Department of Materials Science and Engineering, College of Materials, Xiamen University, Xiamen 361005, P. R. China. E-mail: yuanzhi@xmu.edu.cn, dlpeng@xmu.edu.cn; Fax: +86 592 2183515; Tel: +86-592-2188025*

† Electronic supplementary information (ESI) available: Details of the characterization techniques, XRD patterns, SEM and TEM images, EDS spectra and magnetic data for a portion of samples. See DOI: 10.1039/c3cc45800h

In this communication, Ni–Cu@Au–Cu nanowires with Ni–Cu alloy cores and Au–Cu alloy shells have been obtained using a facile nonaqueous solution method that involves an injection process. Tunable optic and magnetic properties can be achieved by adjusting the percentage of magnetic and plasmonic metal components. In response to the great challenge to coat noble metals over magnetic metal to form a core–shell nanostructure, the strategy revealed in this communication provides a useful hint to construct one-dimensional core–shell nanostructure with both magnetic and plasmonic functionalities.

In a typical synthesis, 0.5 mmol of nickel(II) acetylacetonate ($Ni(acac)_2$) and 0.3 mmol of copper(II) chloride dehydrate ($CuCl_2{\cdot}2H_2O$) were added in 5 mL of oleylamine and heated to 130 °C for 15 min. After cooling to room temperature, the mixed solution was then consecutively injected into 6 mL of octadecylene at 185 °C within 1 h *via* an injection pump. After that, the resulted solution was further aged at 210 °C for 1 h and then cooled to 155 °C, at which temperature a solution containing 0.25 g of the premade Au precursor (see ref. 16 for preparation details) dissolved in 2 mL of dichloromethane was quickly injected into the reaction solution. After the rapid injection, the reaction temperature was kept at 140 °C for 1 h and cooled to room temperature. The generated products were washed and separated by repeated precipitation using the mixture of hexane, ethanol and acetone, and then dried in a vacuum. Various characterization techniques were used to analyze the obtained samples (for details see ESI†).

As shown in the low-magnification scanning electron microscopy (SEM) image (Fig. 1a), the as-prepared typical Ni–Cu@Au–Cu nanowires have diameters ranging from 60 to 90 nm (averaged at 75 nm) and lengths of up to tens of micrometers. The transmission electron microscopy (TEM) image (Fig. 1b) of the as-prepared nanowires exhibits nonuniform contrast in the center and edge region, indicating a different composition distribution. The selected area electron diffraction (SAED) pattern (Fig. 1b inset) recorded from randomly distributed nanowires exhibits mixed diffraction rings that can be indexed to Au–Cu and Ni–Cu alloys with a fcc structure. The X-ray diffraction (XRD) pattern (Fig. S1, ESI†) of the as-prepared Ni–Cu@Au–Cu nanowires can also be assigned to the Ni–Cu alloy (JCPDS #09-0205) and the Au–Cu alloy (JCPDS #34-1302) with a fcc

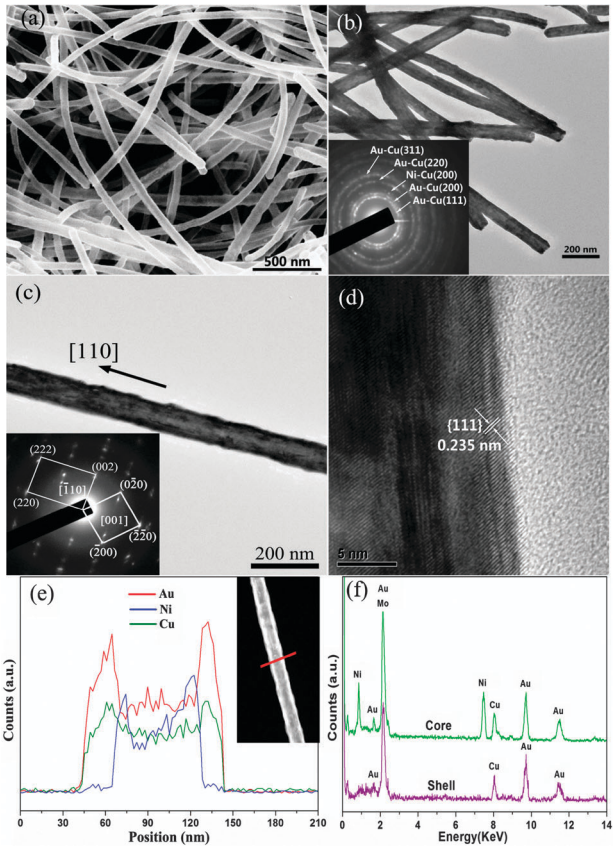


**Fig. 1** Morphological and structural analyses of the typical Ni–Cu@Au–Cu nanowires. (a) SEM image. (b) TEM image with the SAED pattern (inset). (c) A single nanowire with the SAED pattern (inset). (d) HRTEM image. (e) STEM-EDS line-scanning profiles with the HAADF image (inset). (f) EDS spectra from the core and shell positions.

structure. The SAED pattern recorded from a single nanowire (Fig. 1c) exhibits two different diffraction patterns belonging to the [−110] and [001] zone axes, suggesting twinned structures, and a growth direction of [110] is identified. The high-resolution TEM (HRTEM) image (Fig. 1d) recorded from the edge of a nanowire shows lattice fringes corresponding to the {111} planes of the fcc Au–Cu alloy, confirming crystalline nature of the nanowire. The core–shell structure can be revealed from the high-angle annular dark-field (HAADF) image (Fig. 1e inset and Fig. S2, ESI†), in which the thin shell containing Au–Cu alloys obviously looks brighter. The estimated shell thickness is about 9–15 nm. The energy dispersive X-ray spectroscopy (EDS) line-scanning analysis (Fig. 1e) preformed in the scanning TEM (STEM) mode on a single nanowire shows that Au and Cu distribute at the edge while Cu and Ni locate in the center, further confirming a core–shell structure. Fig. 1f shows the typical EDS spectra from a single nanowire. The edge portion shows peaks of Au and Cu with an atomic ratio close to 3 : 1, whereas the center exhibits signals of Ni and Cu (atomic ratio close to 2 : 1) along with Au signals that are contributed from the shell. The above results demonstrate that the as-prepared nanowires have a core–shell structure consisting of a Ni–Cu alloy core and a Au–Cu alloy shell.

The schematic illustration of the formation of a Ni–Cu@Au–Cu nanowire is shown in Fig. 2. At first, Ni atoms that are generated from the reduction of Ni(II) species will rapidly reduce Cu(II) into Cu(0) as well as Ni(0) are oxidized back to Ni(II) *via* a galvanic replacement

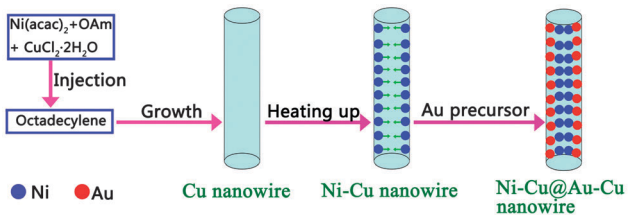


**Fig. 2** Schematic illustration of the formation of Ni–Cu@Au–Cu nanowires.

reaction.[17] The concentration of Cu(0) will increase as the reiteration of the reduction and galvanic replacement proceed, and multi-twinned Cu seeds will be formed rapidly and then develop into Cu nanowires during the injection process. When the temperature rises from 185 to 210 °C, more Ni atoms form and diffuse into Cu nanowires, thus forming Ni–Cu nanowires (Fig. S3 and S4, ESI†). After the injection of the Au precursor, Au monomers begin to nucleate on the surfaces of pre-formed Ni–Cu cores. Au(III) species which may exist due to the incomplete reduction of the Au precursor can oxidize Cu and Ni atoms *via* galvanic replacement reactions, since the redox pair potential of $Au^{3+}$/Au (1.52 V) is higher than that of $Ni^{2+}$/Ni (−0.246 V) and $Cu^{2+}$/Cu (0.337 V), and the generated Cu(II) can also react with Ni atoms. The Cu atoms released from the pre-formed Ni–Cu cores plus the Au atoms generated from the reduction process and galvanic replacement eventually form the Au–Cu alloy shells.

Fig. 3 compares the Visible-Near Infrared (NIR) spectra of the Ni–Cu nanowires (see the TEM image in Fig. S4, ESI†) generated in the intermediate stage and Ni–Cu@Au–Cu nanowires prepared with different contents of the Au precursor. The spectra of the Cu–Ni nanowires (Fig. 3 curve e) show no obvious surface plasmon resonance (SPR) band, which is related to the damping effect of Ni. In contrast, the Ni–Cu@Au–Cu nanowires prepared using 0.15 g (see SEM and TEM images and EDS spectra in Fig. S5, ESI†), 0.25 g, 0.40 g (see SEM and TEM images and EDS spectra in Fig. S6, ESI†) and 0.50 g of the Au precursor (see SEM and TEM images and EDS spectra in Fig. S7, ESI†) show broad SPR bands at around 533, 542, 574 and 600 nm, respectively, which are ascribed to the contribution of Au and Cu that both have a prominent SPR band in the visible range. The SPR frequency is sensitive to the dimension, composition and morphology of plasmonic nanocrystals, which offers convenient ways to tune their optical properties. For example, tunable plasmon resonance frequencies were achieved in Au–Cu alloy nanoparticles by

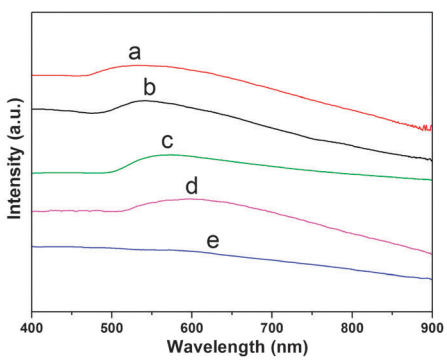


**Fig. 3** Visible-NIR spectra of the Ni–Cu@Au–Cu nanowires prepared using 0.15 g (a), 0.25 g (b), 0.40 g (c) and 0.50 g (d) of the Au precursor, and Ni–Cu nanowires for curve (e).

 

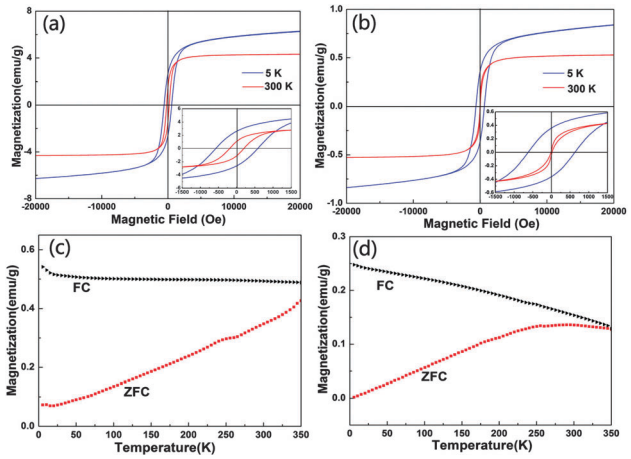


**Fig. 4** Magnetic hysteresis loops (a and b) and ZFC-FC (100 Oe) curves (c and d) of Ni–Cu@Au–Cu nanowires obtained including a step aging at 210 °C for 60 min (a and c) and 195 °C for 60 min (b and d) before the injection of Au precursor.

changing the Cu content.[18] In our case, we find that the Au : Cu ratio is nearly the same (~3 : 1) for all samples, however the sample prepared using 0.5 g of the Au precursor has a larger diameter (~110 nm) than other nanowires, therefore a red-shifted SPR band is resulted. A similar trend was also observed in Au–Cu alloy nanocubes, and the SPR band red shifts as the size of the nanocubes increases.[19]

Since the as-prepared Ni–Cu@Au–Cu nanowires have a magnetic core, we also measured the hysteresis curves and temperature-dependent magnetization curves. The Ni content of the Ni–Cu@Au–Cu nanowires can be controlled by using different reaction temperatures. As shown in Fig. 4a, the corresponding hysteresis loops of the Ni–Cu@Au–Cu nanowire sample obtained including a step aging at 210 °C for 60 min show a ferromagnetic behavior with a coercivity of 579 Oe at 5 K, and a coercivity value of 192 Oe at 300 K. The hysteresis loops of the sample (See SEM and TEM images and EDS spectra in Fig. S8, ESI†) obtained including a step aging at 195 °C for 60 min also exhibit a ferromagnetic characteristic (Fig. 4b). The measured coercivity values are 620 and 15 Oe at 5 and 300 K, respectively. Compared to the normally reported Ni nanoparticles which typically have coercivity values of 200–350 Oe at 5 K,[20,21] or Ni–Cu nanoplates with a close composition,[22] the observed low-temperature (5 K) coercivity values of the Ni–Cu@Au–Cu nanowire samples are much larger. This can be both related to the shape-anisotropic effect and the core–shell interface effect. The one-dimension nanostructure can improve shape-anisotropic energy. In addition, the strain that is created due to the lattice mismatch between Ni–Cu and Au–Cu at the core–shell interface may also pin the Ni spin rotations and therefore enhance the coercivity. The observed higher saturation magnetization values of the sample obtained at 210 °C may correlate with the relatively higher content of Ni. The zero-field cooled (ZFC) and field cooled (FC) curves of the Ni–Cu@Au–Cu nanowires obtained at 210 °C and 195 °C are presented in Fig. 4c and d, respectively. For the sample obtained at 210 °C, the estimated blocking temperature ($T_B$) from the ZFC curve is beyond 350 K, while that of the sample obtained at 195 °C is about 290 K. It is possible that the improved shape-anisotropic energy for the nanowires may contribute to the higher divergence temperature of the magnetization in the ZFC-FC measurements. The values of $T_B$ for the samples obtained at 185 °C (Fig. S9 and S11, ESI†) and 205 °C (Fig. S10 and S11, ESI†) are about 200 K and near 350 K, respectively. Therefore, the magnetic properties of Ni–Cu@Au–Cu nanowires are tunable and the possessed ferromagnetic properties enable them to be easily recycled after use in solution when an external magnetic field is applied.

Attempts have also been made to synthesize Ni–Cu nanowire cores *via* a one-pot reaction at first and then add the Au precursor to obtain alloy shells. However, the products usually contain some nanoparticles (see Fig. S12, ESI†). A possible reason is that the one-pot synthesis readily incurs a high concentration of nuclei which may not fully develop in the later stage. However in the injection approach, the nuclei concentration at the beginning stage is restricted by the delivering rate. A relatively low concentration of nuclei along with the continuous delivery of source materials can help nuclei develop into one-dimensional nanostructure, thus improving the shape singularity.

In summary, we demonstrate a nonaqueous injection method for the preparation of a one-dimensional alloy core–shell nanostructure (Ni–Cu@Au–Cu) that possesses both magnetic and plasmonic functionalities. The as-synthesized Ni–Cu@Au–Cu nanowires can serve as magnetic–plasmonic hybrids for the fundamental understanding of the interplay between different components and find applications in diverse technological fields.

The authors gratefully acknowledge financial support from the National Basic Research Program of China (No. 2012CB933103), the National Outstanding Youth Science Foundation of China (Grant No. 50825101), and the National Natural Science Foundation of China (Grant Nos. 51171157 and 51171158).

## Notes and references

1 D. Wang and Y. Li, *Adv. Mater.*, 2011, **23**, 1044.
2 J.-M. Yan, X.-B. Zhang, T. Akita, M. Haruta and Q. Xu, *J. Am. Chem. Soc.*, 2010, **132**, 5326.
3 H.-L. Jiang, T. Akita and Q. Xu, *Chem. Commun.*, 2011, **47**, 10999.
4 D. L. Feldheim and C. D. Keating, *Chem. Soc. Rev.*, 1998, **27**, 1.
5 A. R. Rathmell, M. Nguyen, M. Chi and B. J. Wiley, *Nano Lett.*, 2012, **12**, 3193.
6 J. Guo, X. Wang, P. Miao, X. Liao, W. Zhang and B. Shi, *J. Mater. Chem.*, 2012, **22**, 11933.
7 P. K. Sudeep, S. T. S. Joseph and K. G. Thomas, *J. Am. Chem. Soc.*, 2005, **127**, 6516.
8 J. Cheon and J.-H. Lee, *Acc. Chem. Res.*, 2008, **41**, 1630.
9 C. Sun, J. S. H. Lee and M. Zhang, *Adv. Drug Delivery Rev.*, 2008, **60**, 1252.
10 S. Zhang and H. C. Zeng, *Chem. Mater.*, 2010, **22**, 1282.
11 Z. Liu, D. Elbert, C. L. Chien and P. C. Searson, *Nano Lett.*, 2008, **8**, 2166.
12 M. Wen, B. Sun, B. Zhou, Q. Wu and J. Peng, *J. Mater. Chem.*, 2012, **22**, 11988.
13 P. R. Sajanlal and T. Pradeep, *Nanoscale*, 2012, **4**, 3427.
14 M. McKiernan, J. Zeng, S. Ferdous, S. Verhaverbeke, K. S. Leschkies, R. Gouk, C. Lazik, M. Jin, A. L. Briseno and Y. Xia, *Small*, 2010, **17**, 1927.
15 S. Lin, S. Chen, Y. Chen and S. Cheng, *J. Alloys Compd.*, 2008, **449**, 232.
16 H. She, Y. Chen, X. Chen, K. Zhang, Z. Wang and D.-L. Peng, *J. Mater. Chem.*, 2012, **22**, 2757.
17 H. Guo, Y. Chen, H. Ping, J. Jin and D. L. Peng, *Nanoscale*, 2013, **5**, 2394.
18 N. E. Motl, E. Ewusi-Annan, I. T. Sines, L. Jensen and R. E. Schaak, *J. Phys. Chem. C*, 2010, **114**, 19263.
19 Y. Liu and A. R. Walker, *Angew. Chem., Int. Ed.*, 2010, **122**, 6933.
20 Y. Chen, D.-L. Peng, D. Lin and X. Luo, *Nanotechnology*, 2007, **18**, 505703.
21 H. T. Zhang, G. Wu, X. H. Chen and X. G. Qiu, *Mater. Res. Bull.*, 2006, **41**, 495.
22 H. Guo, Y. Chen, H. Ping, L. Wang and D.-L. Peng, *J. Mater. Chem.*, 2012, **22**, 8336.